Research paper

Cite as: Batis V, Detorakis E, Schiza S, Prokopakis E, Krasagakis K, Drakonaki E: Ultrasound imaging in floppy eyelid syndrome: anatomical and clinical considerations. J Ultrason 2025; 25: 19. doi: 10.15557/JoU.2025.0019.

Submitted: 16.03.2025
Accepted: 10.06.2025
Published: 30.06.2025

Ultrasound imaging in floppy eyelid syndrome: anatomical and clinical considerations

Vasilios Batis[1], Efstathios Detorakis[1], Sophia Schiza[2], Emmanuel Prokopakis[3], Konstantinos Krasagakis[4], Elena Drakonaki[5]

[1] *Department of Ophthalmology, School of Medicine, University of Crete, Greece*
[2] *Department of Respiratory Medicine and Sleep Disorders Unit, School of Medicine, University of Crete, Greece*
[3] *Department of Otorhinolaryngology and Laboratory of Translational Otorhinolaryngology Research, School of Medicine, University of Crete, Greece*
[4] *Department of Dermatology, Medical School, University of Crete, Greece*
[5] *Department of Anatomy, School of Medicine, University of Crete, Greece*

Corresponding author: Elena Drakonaki; e-mail: drakonaki@yahoo.gr

DOI: 10.15557/JoU.2025.0019

Keywords
high-frequency skin ultrasound; strain elastography; shear wave elastography; floppy eyelid

Abstract

Aim of the study: Skin ultrasonography and elastography provide information on superficial tissue anatomy and elasticity. Floppy eyelid syndrome is characterized by eyelid hyperlaxity and is associated with several ophthalmic and systemic conditions, such as obstructive sleep apnea. This study evaluates the diagnostic role of ultrasonography and elastography in floppy eyelid syndrome. **Methods:** This is a prospective case-control study. Patients were recruited from the Oculoplastic Service of the Department of Ophthalmology at the University Hospital of Heraklion, Crete, Greece. The diagnosis of floppy eyelid syndrome was based on the eversion of the upper eyelid upon unassisted digital traction. Cataract surgery candidates without floppy eyelid syndrome were consecutively recruited as controls. Patients with a history of previous eyelid pathology or surgery were excluded. Ultrasound examination was performed using high-frequency linear probes (GE E9) for B-mode imaging and shear wave and strain elastography. Upper airway measurements included tongue thickness and upper airway length. Clinical and demographic findings were recorded. **Results:** Twenty-eight patients were included (14 with floppy eyelid syndrome, 14 controls). Orbicularis muscle elasticity in kPa was significantly higher in the floppy eyelid syndrome group, compared with controls (independent samples t-test score 2.64, $p = 0.04$). Tongue thickness and upper airway length were also significantly correlated with several eyelid B-mode and elastography parameters in patients with floppy eyelid syndrome, including subcutaneous fat and orbicularis muscle thickness and elasticity. **Conclusions:** Findings from this feasibility study imply that ultrasound and elastography parameters may be used in the evaluation of floppy eyelid syndrome and support an association between eyelid elasticity and upper airway anatomical parameters in this condition.

Introduction

Floppy eyelid syndrome (FES) is characterized by eyelid hyperlaxity, and was initially described by Culbertson and Ostler in 1981[1] as the spontaneous eversion of the upper eyelids[1–3]. Histopathological studies have revealed a significant decrease in elastin content in the eyelids of patients with FES[4]. Moreover, significant associations between FES and systemic conditions, such as obstructive sleep apnea (OSA), obesity, connective tissue disorders, and Down syndrome, have been reported[5,6].

High-frequency ultrasound imaging of the skin (HFUS), with frequencies greater than 15 MHz, allows high-resolution imaging of all layers of facial skin[7]. In recent years, the technique of ultrasound elastography (USE) has also been added to map tissue elasticity, either qualitatively (strain elastography, SE)[8] or both qualitatively and quantitatively (shear wave elastography, SWE)[9–12]. Moreover, upper respiratory tract ultrasonography has been used for the diagnosis and grading of severity in OSA[13,14]. This study investigates the potential role of HFUS and USE as imaging modalities for the upper eyelid and upper respiratory tract in FES, and examines clinical and demographic correlations.

Materials and methods

This is a prospective case-control study. Approval from the Ethics Review Board of the Medical School of the University of Crete was obtained, and the study adhered to the ethical principles outlined in the Declaration of Helsinki, as amended in 2013. All patient-identifying information was removed from figures, and all participants signed an informed consent form for participation in the study.

Patients with bilateral FES were consecutively recruited from the Oculoplastic Service of the Department of Ophthalmology at the University Hospital of Heraklion. Consecutively examined cataract surgery candidates without FES were recruited as controls. Inclusion criteria were adult patients capable of giving informed consent. FES diagnosis was based on the unassisted digital eversion of the upper eyelid, which then remained everted for up to 6 seconds (FES stage 1) or more than 6 seconds (FES stage 2), despite downgaze or voluntary contraction of the orbicularis oculi muscle, as previously described[15]. Exclusion criteria were minors, patients who had undergone surgical interventions in the examined anatomical structures, patients under prostaglandin anti-glaucomatous medications, contact lens users, and patients with upper respiratory tract pathologies or periocular pathologies other than FES. The demographic and clinical variables recorded included age, gender, weight, height, body mass index (BMI), smoking status, and use of positive airway pressure (PAP).

HFUS and USE examinations were performed with the ultrasound probe placed on the gel-covered preseptal and pretarsal right upper eyelid and neck skin, without pressure, using a single US system (LOGIQ E9 system, Software Version R5; GE Healthcare, Milwaukee, WI), by a single radiologist with 17 years of experience in US elastography (ED), who was blinded to the classification of participants.

For HFUS, a high-frequency (8–18 MHz) linear array "hockey stick" transducer and the standard "MSK superficial" setting were used. Layers identified from superficial to deep were:

1. the most superficial hyperechoic epidermis-dermis layer, including the sub-epidermal low echogenicity band (SLEB);
2. the inhomogeneous hypodermis subcutaneous layer;
3. the palpebral part of the orbicularis oculi muscle.

The segmentation of the respective layers and placement of the ultrasound probe over the upper eyelid are presented in Fig. 1. The anteroposterior diameter (thickness) of each layer, in mm, was measured in zoom mode. Parameters recorded included the epidermis-dermis thickness (EDT), subcutaneous fat thickness (SFT), and orbicularis oculi muscle thickness (OOT).

For SE, a high-frequency linear array transducer (ML6–15, frequency range 4–15 MHz) and the standard "MSK superficial" setting of the manufacturer were used. The compression-relaxation cycles included one or two compressions per second, and only circles with the correct level of compression were selected by checking the pressure indicator bar on the screen. The elastogram appeared within a rectangular region of interest (ROI), including all the soft tissue layers of the upper eyelid, displayed side by side with the respective B-mode image. Color mapping for each pixel inside the ROI was displayed relative to the degree of strain of all the tissues within the ROI. Red color represented the softest tissue, while green and blue represented the intermediate and hardest components inside the ROI, respectively. Tissue-specific parameters included the elasticity ratio of the upper eyelid epidermis and dermis relative to subcutaneous fat (skin-to-subcutaneous fat ratio, SFR), and the elasticity ratio of the orbicularis oculi muscle to subcutaneous fat (orbicularis oculi-to-fat ratio, OFR) (Fig. 2).

SWE was performed using a linear transducer (9L, 2–8 MHz). Using time-interleaved shear wave tracking, the shear wave velocity was measured, and subsequently the Young's elastic modulus in kilopascals (kPa) was automatically calculated by the system's built-in software. A rectangular ROI was placed to include the upper eyelid soft tissue. A color-coded SWE value image, superimposed on the conventional B-mode image and displayed side by side with

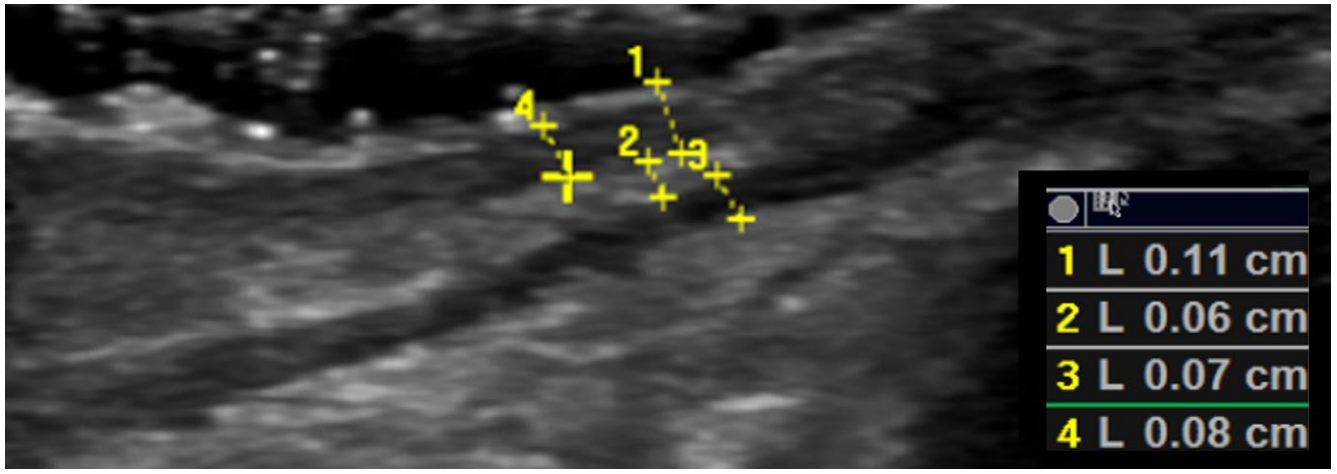

Fig. 1. *Segmentation of upper eyelid anatomical layers in high-frequency ultrasound imaging of the skin (HFUS). HFUS image of the upper eyelid using a high-frequency (8–18 MHz) linear array hockey stick transducer and the standard "MSK superficial" setting of the manufacturer, showing the anatomical layers of the eyelid soft tissue. The thickness of each layer is measured using the system's built-in software tool (calipers) as follows: Measurement 1: Thickness of the most superficial epidermis-dermis layer thickness (EDT), extending from the skin surface to the subcutaneous layer, including the subepidermal low echogenicity band (SLEB). Measurement 2: Thickness of the hyperechoic subcutaneous layer, extending from the deep SLEB to the surface of the underlying muscle (SFT). Measurement 3: Thickness of the palpebral part of the orbicularis oculi muscle, demonstrated as hypoechoic linear muscle fibers (OOT). Measurement 4: Thickness of the SLEB, presenting as a thin band of lower echogenicity at the deepest part of the epidermis-dermis layer*

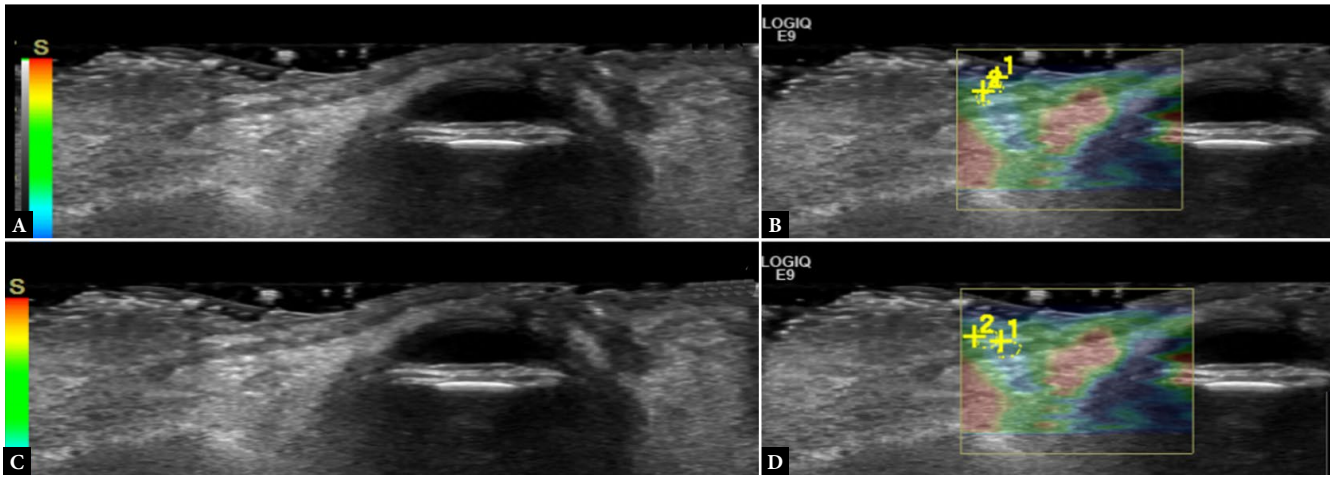

Fig. 2. *Strain elastography (SE) of the upper eyelid.* **A**, **B.** *Epidermis and dermis layer. B-mode image (***A***) and corresponding elastography image (***B***), with color code showing the elasticity scale. The elasticity ratio of the upper eyelid epidermis and dermis layer relative to the subcutaneous fat (skin-to-subcutaneous fat ratio, SFR, A/B) is measured using manually applied ROIs located in the skin (1) and in the fat (2). The respective elasticity values and ratio are automatically calculated and displayed on the screen.* **C**, **D.** *Orbicularis oculi muscle layer. B-mode image (***C***) and corresponding elastography image (***D***), with color code showing the elasticity scale. The elasticity ratio of the orbicularis oculi muscle layer to subcutaneous fat (orbicularis-to-fat ratio, OFR, A/B) is measured using manually applied ROIs located in the muscle (1) and in the fat (2). The respective elasticity values and ratio are automatically calculated and displayed on the screen*

it on screen, was created. Stiff areas (high kPa) were presented as red, and soft areas (low kPa) as blue. To avoid misregistration, several SWE cycles were performed. The cine loops were reviewed, and only the elastograms in which >80% of the ROI was color-coded and the color pattern remained constant were used to obtain the measurements. The measurement of the SWE values was performed using equally sized circular ROIs manually placed on the lower eyelid skin, subcutaneous fat, and muscle. Three measurements were obtained for each tissue layer, and the mean elasticity value (in kPa) was recorded, including the epidermis-dermis layer (ESW), subcutaneous fat tissue layer (FSW), and orbicularis oculi muscle layer (OSW) (Fig. 3).

Ultrasonographic anatomical imaging of the oropharynx was performed according to previously described protocols[13,14]. To image the base of the tongue, a linear 2–8 MHz transducer was placed along the coronal and sagittal planes. On the coronal plane, the transducer was tilted slightly posteriorly and cephalad to identify the base of the tongue, including, from superficial to deep: a) the acoustic shadow of the hyoid bone; b) the heterogenous hypoechoic muscle fiber complex consisting of the intrinsic muscle fibers and the extrinsic genioglossus muscle; and c) the echogenic mucosal layer. On this plane (coronal plane), tongue thickness (TT) was measured as the anteroposterior diameter between the echogenic mucosa and the shadow of the hyoid. Subsequently, the transducer was rotated into the longitudinal plane at the midline of the neck to obtain a sagittal image of the base of the tongue, in which the same layers could be identified[14], including, from superficial to deep: (a) the deepest geniohyoid muscle running between the shadow of the hyoid and the mandible; (b) the fan-like genioglossus muscle; (c) the intrinsic muscle deep to the mucosa; and (d) the echogenic mucosa. On this plane (sagittal plane), the upper airway length (UAL) was measured as the anteroposterior diameter between the anterior edge of the hyoid bone and the hyperechoic line corresponding to the air column at the edge of the hard palate[13] (Fig. 4).

Statistical analysis

All statistical analyses were performed using SPSS version 13.0 (Chicago, IL, USA). Normality tests (Kolmogorov-Smirnov and Shapiro-Wilk tests) were performed for the continuous variables. Statistical criteria employed included independent samples t-tests, Pearson's chi-square tests, and Pearson's bivariate correlation analysis. Non-parametric criteria, such as the Mann-Whitney U test, were planned to be employed if variables did not follow a normal distribution. Statistical significance was set at $p < 0.05$.

Results

Twenty-eight patients (28 eyelids) were included in the study (14 with FES and 14 controls). In the FES group, there were 12 males and 2 females, whereas in the control group there were 9 males and 5 females ($p > 0.05$, Pearson's chi-square test). In the FES group, there were 9 smokers and 5 non-smokers, whereas in the control group there were 7 smokers and 7 non-smokers ($p > 0.05$, Pearson's chi-square test). In the FES group, 4 patients reported PAP use, whereas the respective number in the control group was 1 patient; the difference was statistically significant (Pearson's chi-square test value 4.38, $p = 0.03$). Nine (64.28%) of the FES patients were classified as stage 1 and 5 (35.71%) as stage 2. The distribution of age, weight, height, and BMI was normal (Kolmogorov-Smirnov and Shapiro-Wilk tests), and differences in age, weight, height, and BMI between the FES and control groups were also statistically not significant (independent samples t-test) (Tab. 1).

Upper eyelid HFUS and USE measurements for both the FES and control groups, along with levels of statistical significance for the respective differences are presented in Tab. 2. All tissue measurement parameters for the upper eyelid tested followed a normal distribution (Kolmogorov-Smirnov and Shapiro-Wilk tests). Concerning HFUS measurements, although EDT, SFT, and OOT scores were

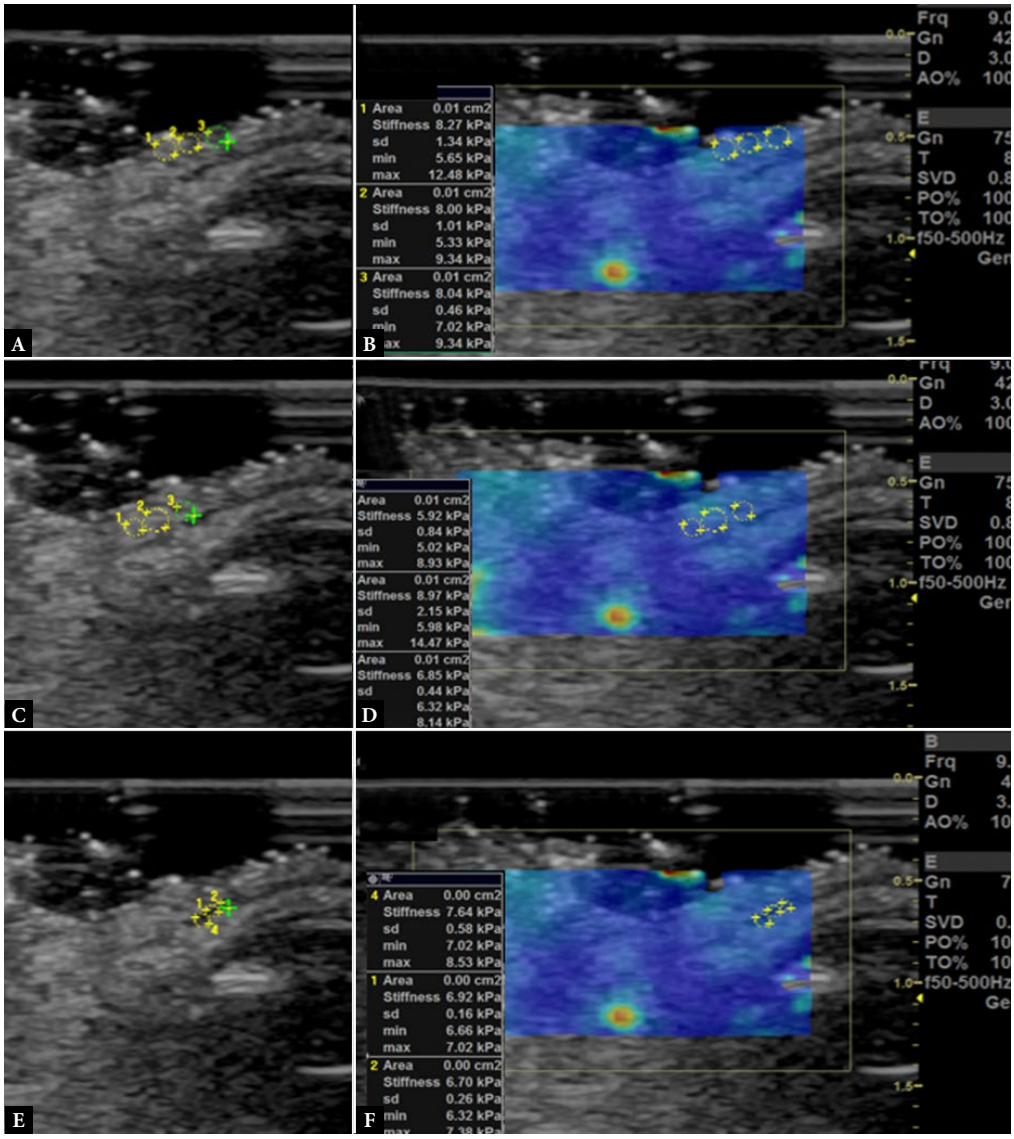

Fig. 3. *Shear wave elastography (SWE) of the upper eyelid.* **A**, **B.** *Superficial epidermis-dermis layer. B-mode image (***A***) and superimposed SWE color coded image showing the elasticity scale (***B***). Three SWE measurements are performed using circular ROIs manually placed on the imaged area. The quantitative assessment of elasticity in kPa (mean value, maximum, minimum, standard deviation) is presented in a superimposed table.* **C**, **D.** *Subcutaneous fat layer. B-mode image (***C***) and superimposed SWE color-coded image showing the elasticity scale (***D***). Three SWE measurements are performed using circular ROIs manually placed on the subcutaneous fat layer. The quantitative assessment of elasticity in kPa (mean value, maximum, minimum, standard deviation) is presented in a superimposed table.* **E**, **F.** *Orbicularis oculi muscle layer. B-mode image (***E***) and superimposed SWE color-coded image showing the elasticity scale (***F***). Three SWE measurements are performed using circular ROIs manually placed on the orbicularis oculi muscle. The quantitative assessment of elasticity in kPa (mean value, maximum, minimum, standard deviation) is presented in a superimposed table. In all cases, only the mean value was used for statistical analysis*

Tab. 1. Descriptive statistics for clinical and demographic parameters (mean ± SD, range) for FES and control groups, with independent samples t-test scores and associated levels of statistical significance

Parameter	FES mean ± SD (range)	Controls mean ± SD (range)	Independent samples t-test	*p*
Age (years)	65.64 ± 12.9 (40–88)	59.21 ± 14.21 (20–78)	0.41	0.15
Weight (kg)	93.50 ± 25.0 (64–140)	91.00 ± 23.13 (52–135)	0.38	0.69
Height (cm)	1.69 ± 0.08 (1.55–1.87)	1.71 ± 0.12 (1.50–1.87)	0.15	0.53
BMI	32.13 ± 6.71 (25–49.93)	30.63 ± 6.23 (23.11–42.60)	0.48	0.39
FES – floppy eyelid syndrome				

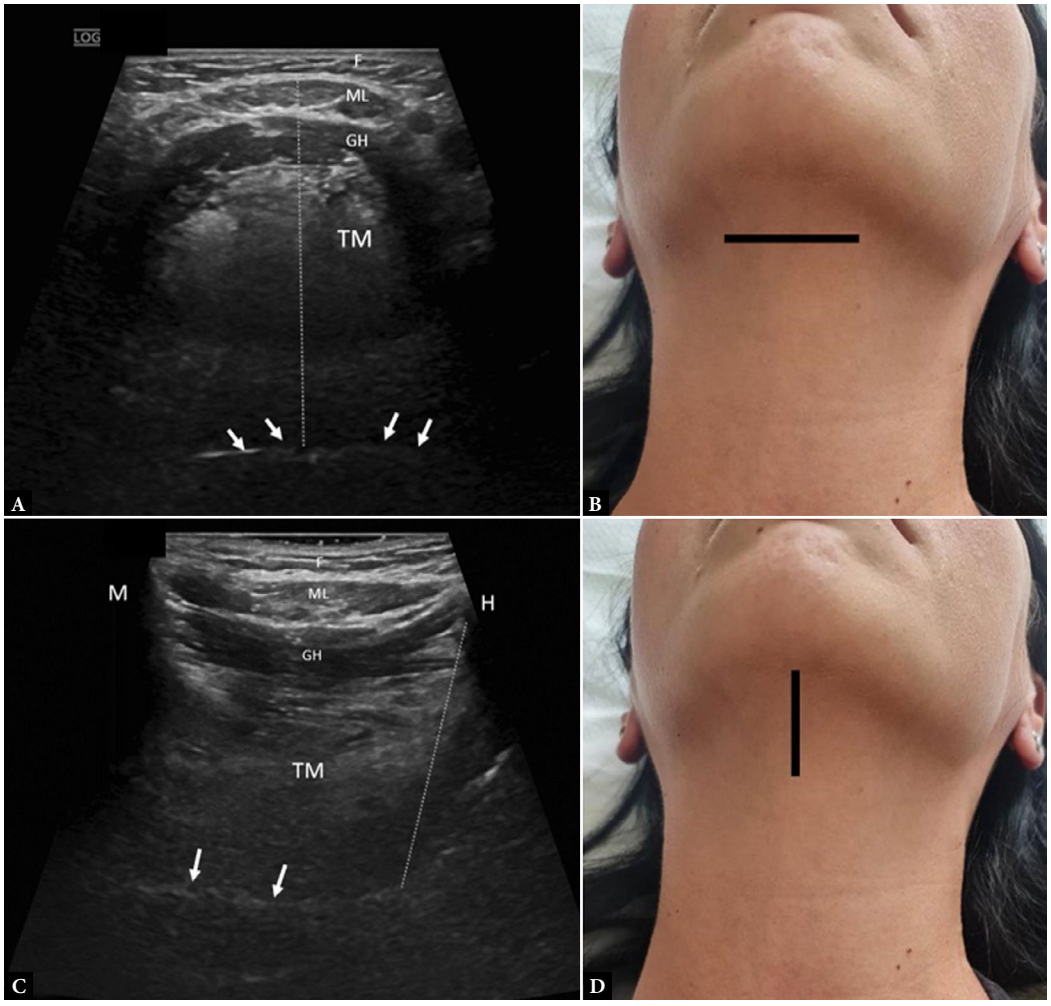

Fig. 4. A. *Tongue thickness (TT) measurement as the anteroposterior diameter between the echogenic mucosa (arrow) and the surface of the mylohyoid muscle (ML) at the floor of the mouth (dotted line).* **B.** *Corresponding placement of the ultrasound probe over the neck area. GH – geniohyoid; TM – intrinsic and extrinsic (genioglossus) muscles of the tongue, ML – mylohyoid muscle; F – subcutaneous fat.* **C.** *Upper airway length (UAL) measurement as the anteroposterior diameter between the anterior edge of the hyoid bone (H) and the hyperechoic line corresponding to the air column at the edge of the hard palate (arrows)* (**D**) *respective placement of the ultrasound probe over the neck area. GH – geniohyoid; TM – intrinsic and extrinsic (genioglossus) muscles of the tongue; ML – mylohyoid muscle; F – subcutaneous fat; H – hyoid bone shadow; M – mandible shadow*

Tab. 2. Upper eyelid and submental tissue USE, SE, and SWEI parameter measurements (mean ± SD, range), with associated levels of statistical significance

Parameter	FES mean ± SD (range)	Controls mean ± SD (range)	Independent samples t-test	*p*
EDT (mm)	0.11 ± 0.08 (0.06–0.53)	0.09 ± 0.03 (0.06–0.14)	8.66	0.09
SFT (mm)	0.09 ± 0.03 (0.03–0.20)	0.07 ± 0.03 (0.04–0.12)	2.12	0.74
OOT (mm)	0.10 ± 0.03 (0.05–0.14)	0.09 ± 0.04 (0.05–0.18)	3.77	0.14
SFR	1.33 ± 0.85 (0.36–2.70)	1.36 ± 0.83 (0.73–3.38)	–0.10	0.91
OFR	1.05 ± 0.33 (0.53–1.75)	1.12 ± 0.40 (0.63–1.83)	0.67	0.34
ESW (kPa)	11.99 ± 13.3 (2.30–61.21)	6.53 ± 4.80 (3.67–22.00)	0.23	0.97
FSW (kPa)	9.82 ± 8.38 (2.50–38.16)	7.09 ± 4.32 (3.58–19.00)	3.65	0.40
OSW (kPa)	10.81 ± 10.15 (3.02–43.57)	5.00 ± 4.19 (1.45–18.60)	2.64	0.04
TT (cm)	4.37 ± 0.99 (2.83–6.05)	4.33 ± 0.86 (3.60–6.10)	–0.01	0.98
UAL (cm)	3.95 ± 0.80 (2.81–6.05)	5.57 ± 0.78 (2.72–6.45)	–7.68	<0.01

EDT – epidermis-dermis thickness; SFT – subcutaneous fat thickness, OOT – orbicularis oculi thickness; SFR – skin to fat ratio; OFR – orbicularis to fat ratio; ESW – epidermal shear wave, FSW – fat shear wave, OSW – orbicularis shear wave; TT – tongue thickness; UAL – upper airway length

higher in the FES group, only the difference in EDT approached statistical significance (independent samples t-test, $p = 0.09$). Differences in SFR and OFR between the two groups were not statistically significant (independent samples t-test). Regarding SWE measurements, although elasticity values in kPa were higher in the FES group compared with controls, differences in ESW and FSW between the two groups were not statistically significant. In contrast, OSW scores were significantly higher in the FES group compared with the control group (independent samples t-test score 2.64, $p = 0.04$). TT scores did not differ significantly between the FES and control groups, whereas UAL was significantly shorted in the FES group compared with controls (independent samples t-test score −7.68, $p < 0.01$).

Among FES patients, OSW and EDT were significantly higher in patients reporting PAP use (independent samples t-test scores −2.10, $p = 0.04$, and −1.7, $p = 0.04$, respectively). Differences in other HFUS parameters between PAP users and non-users were not statistically significant. Moreover, TT was significantly correlated with SFT and FSW (Pearson's bivariate correlation coefficients 0.594 and 0.376, $p = 0.01$ and $p = 0.04$, respectively) whereas UAL was significantly correlated with SFT, OOT, SFR, ESW, FSW, and OSW with Pearson's bivariate correlation coefficients 0.63 ($p < 0.01$), 0.52 ($p < 0.01$), −0.47 ($p = 0.01$), 0.40 ($p = 0.03$), 0.59 ($p < 0.01$), and 0.45 ($p = 0.01$), respectively. Respective correlations for both TT and UAL in the control group were not statistically significant (Pearson's bivariate correlation coefficient).

Discussion

Previous studies have employed HFUS to study the eyelid and facial skin[16]. However, to the best of our knowledge, this is the first study to employ HFUS for the examination of FES. Moreover, the use of SE and SWE as imaging modalities adds new insights into eyelid biomechanics in FES. Indeed, USE has been extensively used to examine tissue elasticity in several organs and conditions, including ocular and periocular tissues[10,17–21]. Although the thicknesses of the skin, subcutaneous fat, and orbicularis oculi muscles did not differ significantly between FES and controls in this study, the elasticity of the orbicularis muscle, as measured by SWE, was significantly lower in FES, implying a possible role of SWE in the study of FES. Importantly, the fact that the majority of FES patients were classified as early (stage 1) cases implies that SWE may assist in the diagnosis of early or subclinical forms of FES. The increased stiffness of the orbicularis oculi muscle in FES is consistent with the fact that elastin is markedly decreased in both the tarsus and the pretarsal orbicularis of FES patients, implying that elastin is the main culprit in FES[22,23]. Indeed, previous studies have reported a strong association between decreased elastin content and decreased elasticity in tissues[24].

The lack of a statistically significant association between FES and BMI is also in accordance with previous studies, which have reported FES in non-obese persons[25–27]. In contrast, there is strong literature support for the association between FES and OSA[25,28], which is also in agreement with findings from this study, since PAP use was significantly more common in FES. A potential underlying link between FES and OSA is supported by fact that, among FES patients, OSW and EDT were significantly higher in those reporting PAP use. The fact that ultrasonographic examinations are non-invasive, safe, quick, and easy to perform implies that they could be used as ophthalmic imaging biomarkers for the early detection of OSA. Moreover, the fact that upper respiratory tract ultrasound anatomical measurements such as TT and UAL, which are closely linked to the diagnosis of OSA[13,14], were significantly correlated with HFUS eyelid parameters, including SFT and FSW and SFT, OOT, SFR, ESW, FSW, and OSW (for TT and UAL respectively), supports the concept that the eyelid and upper respiratory tract tissues share similar properties and may suffer from similar biomechanical defects. Common pathogenetic pathways between FES and OSA have been previously described, resulting from hypoxia-derived oxidative stress, including abnormalities in elastin fibers associated with increased levels of metalloproteinases, leading to changes in tarsal elasticity and laxity of the lateral canthal tendons[29]. The selection of UAL and TT as metrics of upper respiratory tract anatomy was based on the fact that they are directly associated with airway volume, rather than tissue volume, such as the volume of the tonsils, which is more likely to correlate with BMI than with OSA severity[30].

The small number of cases is a weakness of this study, which could have an impact on the robustness of the results. Another limitation concerning the upper respiratory tract images is that anatomical measurements in the sagittal and coronal planes may be challenging to acquire, especially in obese individuals, in whom sonoanatomy is less evident unless low frequencies are used (8–9 MHz). However, the fact that the design of the study was prospective and that all ultrasonographic examinations were performed using the same protocol and ultrasonographic platform, and by the same experienced radiologist who was blinded to patient classification, strengthens the validity of the findings. Moreover, the fact that several exclusion criteria were applied, including factors that could potentially affect ultrasonographic and elastographic outcomes, implies that the findings are likely to be directly associated with FES and may be added as non-invasive and easy-to-use diagnostic modalities and in raising clinical suspicion of concomitant OSA. As this was designed as a feasibility study for the application of ultrasonography in the evaluation of FES patients, further studies are needed to validate the results and explore the implications in clinical practice.

Conclusions

High-frequency ultrasonographic imaging, as well as strain and shear wave ultrasound elastography, may serve as imaging modalities for studying floppy eyelid syndrome and exploring its associations with upper airway anatomy, potentially assisting in the diagnosis of obstructive sleep apnea.

Conflict of interest

The authors do not report any financial or personal connections with other persons or organizations, which might negatively affect the contents of this publication and/or claim authorship rights to this publication.

Author contributions

Original concept of study: EDt. Writing of manuscript: VB, EDt, EDk. Analysis and interpretation of data: VB, EDk. Final acceptation of manuscript: VB, EDt, SS, EP, KK, EDk. Collection, recording and/or compilation of data: VB, SS, EDk. Critical review of manuscript: VB, EDt, SS, EP, EDk.

References

1. Culbertson WW, Ostler HB: The floppy eyelid syndrome. Am J Ophthalmol 1981; 92: 568–575. doi: 10.1016/0002-9394(81)90652-8.
2. Salinas R, Puig M, Fry CL, Johnson DA, Kheirkhah A: Floppy eyelid syndrome: A comprehensive review. Ocul Surf 2020; 18: 31–39. doi: 10.1016/j.jtos.2019.10.002.
3. Goldberg R, Seiff S, McFarland J, Simons K, Shorr N: Floppy eyelid syndrome and blepharochalasis. Am J Ophthalmol 1986; 102: 376–381. doi: 10.1016/0002-9394(86)90014-0.
4. Netland PA, Sugrue SP, Albert DM, Shore JW.: Histopathologic features of the floppy eyelid syndrome. Involvement of tarsal elastin. Ophthalmology 1994; 101: 174–181. doi: 10.1016/s0161-6420(94)31368-6.
5. Huon LK, Liu SY, Camacho M, Guilleminault C: The association between ophthalmologic diseases and obstructive sleep apnea: a systematic review and meta-analysis. Sleep Breath 2016; 20: 1145–1154. doi: 10.1007/s11325-016-1358-4.
6. De Gregorio A, Cerini A, Scala A, Lambiase A, Pedrotti E, Morselli S: Floppy eyelid, an under-diagnosed syndrome: a review of demographics, pathogenesis, and treatment. Ther Adv Ophthalmol 2021; 13: 25158414211059247. doi: 10.1177/25158414211059247.
7. Levy J, Barrett DL, Harris N, Jeong JJ, Yang X, Chen SC: High-frequency ultrasound in clinical dermatology: a review. Ultrasound J 2021; 13: 24. doi: 10.1186/s13089-021-00222-w.
8. Detorakis ET, Drakonaki EE, Tsilimbaris MK, Pallikaris IG, Giarmenitis S: Real-time ultrasound elastographic imaging of ocular and periocular tissues: a feasibility study. Ophthalmic Surg Lasers Imaging 2010; 41: 135–141. doi: 10.3928/15428877-20091230-24.
9. Bontzos G, Douglas VP, Douglas KAA, Kapsala Z, Drakonaki EE, Detorakis ET: Ultrasound elastography in ocular and periocular tissues: a review. Curr Med Imaging 2021; 17: 1041–1053. doi: 10.2174/1573405616666201214123117.
10. Douglas KA, Drakonaki EE, Douglas VP, Detorakis ET: Shear-wave elastographic imaging in choroidal melanomas: clinical and hemodynamic correlations. Jpn J Ophthalmol 2024; 68: 523–530. doi: 10.1007/s10384-024-01086-y.
11. Sigrist RMS, Liau J, Kaffas AE, Chammas MC, Willmann JK: Ultrasound elastography: review of techniques and clinical applications. Theranostics 2017; 7: 1303–1329. doi: 10.7150/thno.18650.
12. Meng Y, Feng L, Shan J, Yuan Z, Jin L: Application of high-frequency ultrasound to assess facial skin thickness in association with gender, age, and BMI in healthy adults. BMC Med Imaging 2022; 22: 113. doi: 10.1186/s12880-022-00839-w.
13. Shu CC, Lee P, Lin JW, Huang CT, Chang YC, Yu CJ, Wang HC: The use of submental ultrasonography for identifying patients with severe obstructive sleep apnea. PLoS One 2013; 8: e62848. doi: 10.1371/journal.pone.0062848.
14. Coquia SF, Hamper UM, Holman ME, DeJong MR, Subramaniam RM, Aygun N, Fakhry C: Visualization of the oropharynx with transcervical ultrasound. AJR Am J Roentgenol 2015; 205: 1288–1294. doi: 10.2214/AJR.15.14299.
15. Beis PG, Brozou CG, Gourgoulianis KI, Pastaka C, Chatzoulis DZ, Tsironi EE: The floppy eyelid syndrome: evaluating lid laxity and its correlation to sleep apnea syndrome and body mass index. ISRN Ophthalmol 2012; 2012: 650892. doi: 10.5402/2012/650892.
16. Chen G, Leng X, Liu W, Meng J, Liao X: High-frequency ultrasound findings of sebaceous carcinoma in the eyelid. Skin Res Technol 2024; 30: e13555. doi: 10.1111/srt.13555.
17. Santos R, Valamatos MJ, Mil-Homens P, Armada-da-Silva PAS: Effect of Knee Angle, Contractile Activity, and Intensity of Force Production on Vastus Lateralis Stiffness: A Supersonic Shear Wave Elastography Pilot Study. Sports (Basel) 2024; 12: 211. doi: 10.3390/sports12080211.
18. Xu R, Ren L, Zhang X, Qian Z, Wu J, Liu J, Li Y, Ren L: Non-invasive *in vivo* study of morphology and mechanical properties of the median nerve. Front Bioeng Biotechnol 2024; 12: 1329960. doi: 10.3389/fbioe.2024.1329960.
19. McCormack B, Hampton HL, Speich JE, Radley SC, Burkett LS, Klausner AP: Ultrasound urodynamics: a review of ultrasound imaging techniques for enhanced bladder functional diagnostics. Curr Bladder Dysfunct Rep 2024; 19: 263–271. doi: 10.1007/s11884-024-00758-2.
20. Skrip LM, Moosburner S, Tang P, Guo J, Görner S, Tzschätzsch H, et al.: Viscoelastic properties of colorectal liver metastases reflect tumour cell viability. J Transl Med 2024; 22: 774. doi: 10.1186/s12967-024-05559-z.
21. Ma S, Zhang Z, Li GY, Cao Y: Guided wave elastography of human skins with a layered model incorporating the effect of muscle state. J Biomech 2024; 174: 112279. doi: 10.1016/j.jbiomech.2024.112279.
22. Netland PA, Sugrue SP, Albert DM, Shore JW: Histopathologic features of the floppy eyelid syndrome. Involvement of tarsal elastin. Ophthalmology 1994; 101: 174–181. doi: 10.1016/s0161-6420(94)31368-6.
23. Klapper SR, Jordan DR. Floppy eyelid syndrome. Ophthalmology 1998; 105: 1582. doi: 10.1016/S0161-6420(98)99017-0
24. Naya Y, Takanari H: Elastin is responsible for the rigidity of the ligament under shear and rotational stress: a mathematical simulation study. J Orthop Surg Res 2023; 18: 310. doi: 10.1186/s13018-023-03794-6.
25. Beis PG, Brozou CG, Gourgoulianis KI, Pastaka C, Chatzoulis DZ, Tsironi EE: The floppy eyelid syndrome: evaluating lid laxity and its correlation to sleep apnea syndrome and body mass index. ISRN Ophthalmol 2012; 2012:650892. doi: 10.5402/2012/650892.
26. Paciuc M, Mier ME: A woman with the floppy eyelid syndrome. Am J Ophthalmol 1982; 93: 255–256. doi: 10.1016/0002-9394(82)90429-9.
27. Gross RH, Mannis MJ: Floppy eyelid syndrome in a child with chronic unilateral conjunctivitis. Am J Ophthalmol 1997; 124: 109–110. doi: 10.1016/s0002-9394(14)71654-x.
28. Ezra DG, Beaconsfield M, Sira M, Bunce C, Wormald R, Collin R: The associations of floppy eyelid syndrome: a case control study. Ophthalmology 2010; 117: 831–838. doi: 10.1016/j.ophtha.2009.09.029.
29. Kloosterboer A, Negron CY, Stokkermans TJ: Floppy eyelid syndrome. (Updated 2023 Apr 19). In: StatPearls [Internet]. Treasure Island (FL): StatPearls Publishing; 2025 Jan–.
30. Cahali MB, Soares CF, Dantas DA, Formigoni GG: Tonsil volume, tonsil grade and obstructive sleep apnea: is there any meaningful correlation? Clinics (Sao Paulo). 2011; 66: 1347–1352. doi: 10.1590/s1807-59322011000800007.